P5.3

BIASES IN SURFACE REFERENCE ESTIMATES BY THE TRMM PR STANDARD ALGORITHM

Shinta Seto* and Toshio Iguchi
National Institute of Information and Communications Technology, Tokyo, Japan

1. INTRODUCTION

Attenuation correction is necessary for the accurate rain rate estimation by TRMM/PR, which uses relatively high frequency microwave (13.8GHz) compred with general precipitation radars. The traditional attenuation correction method developed by Hitschfeld and Bordan (HB method) can analytically solve this problem by assuming a k-Z_m relationship such as $k=\alpha Z_m^{\beta}$. However, this method can not be applicable for heavy rainfall. Then, the TRMM/PR standard algorithm (Iguchi et al, 2000) applies hybrid method with HB method and surface reference technique (SRT) (Meneghini et al, 2000). SRT makes use of the return echo by the land surface beyond the precipitation.

The return echo by the land surface is expressed as the land surface backscattering cross section (denoted as σ^0). Due to the attenuation, Measured σ^0 (denoted as σ^0_m) is smaller than actual σ^0 (denoted as σ^0_e) if the observation error is neglected. This difference is PIA (Path Integrated Attenuation), the total attenuation along the path from the radar to surface and its return path. This is written in equation (1). Please note that σ^0 is always expressed in dB unit in this paper.

$$\sigma^0_m = \sigma^0_e - \mathrm{PIA} \quad (1)$$

Under no rain condition,

$$\sigma^0_m(\mathrm{NR}) = \sigma^0_e(\mathrm{NR}) - \mathrm{PIA}(\mathrm{NR}) \quad (2)$$

Under rain condition,

$$\sigma^0_m(\mathrm{R}) = \sigma^0_e(\mathrm{R}) - \mathrm{PIA}(\mathrm{R}) \quad (3)$$

PIA (NR) is attributed to the cloud water and the water vapor, but it is smaller than precipitation attenuation. Then, for simplicity, σ^0_e and PIA are re-defined as follows.

$$\sigma^0_e = \sigma^0_e - \mathrm{PIA}(\mathrm{NR}) \quad (4)$$

$$\mathrm{PIA} = \mathrm{PIA} - \mathrm{PIA}(\mathrm{NR}) \quad (5)$$

* *Corresponding author address*: Shinta Seto, National Institute of Information and Communications Technology, 4-2-1, Koganei, Tokyo, Japan, 184-8795; e-mail: seto@nict.go.jp

Equation (2) can be rewritten into equation (6).

$$\sigma^0_m(\mathrm{NR}) = \sigma^0_e(\mathrm{NR}) \quad (6)$$

Equation (3) still holds. In this way, PIA (NR) is neglected except the case that the absolute value of σ^0_e and PIA is important.

SRT assumes that σ^0_e does not change by the existence of rainfall as described in equation (7).

$$\sigma^0_e(\mathrm{NR}) = \sigma^0_e(\mathrm{R}) \quad (7)$$

From (6) and (7), equation (8) is given.

$$\sigma^0_m(\mathrm{NR}) = \sigma^0_e(\mathrm{R}) \quad (8)$$

In the standard algorithm, SRT selects no-rain pixels which may have similar characteristics with the target pixel and calculates their sample average and standard deviation. The average is used as the estimates of σ^0_e (R) (denoted as σ^0_{ref}). The standard deviation is also used as the reliability factor of the SRT estimates.

$$\mathrm{PIA}_{\mathrm{ref}} = \sigma^0_{ref} - \sigma^0_m(\mathrm{R}) \quad (9)$$

$\mathrm{PIA}_{\mathrm{ref}}$ is the estimates of PIA by the SRT. The final PIA estimates after the hybrid method is denoted as $\mathrm{PIA}_{\mathrm{fin}}$.

The assumption in equation (7) is suspecious. Meneghini et al. (2004) acknowledged that this assumption is sometimes inappropriate. σ^0_e is sensitive to the land surface variables such as surface wind speed over-ocean. The variables can change by the rainfall, however, it is not considered in the SRT of standard algorithm.

Statistical analysis on the change of σ^0_e between under rain condition and under no-rain condition is done in this paper to point out some biases in the SRT of the current standard algorithm.

2. DATA

2.1. Standard Product

The TRMM standard products (2A25, version 6) for the entire year of 2000 are used in the data analysis study in sections 3 to 5. The followings are major variables used in this study from the 2A25 products.

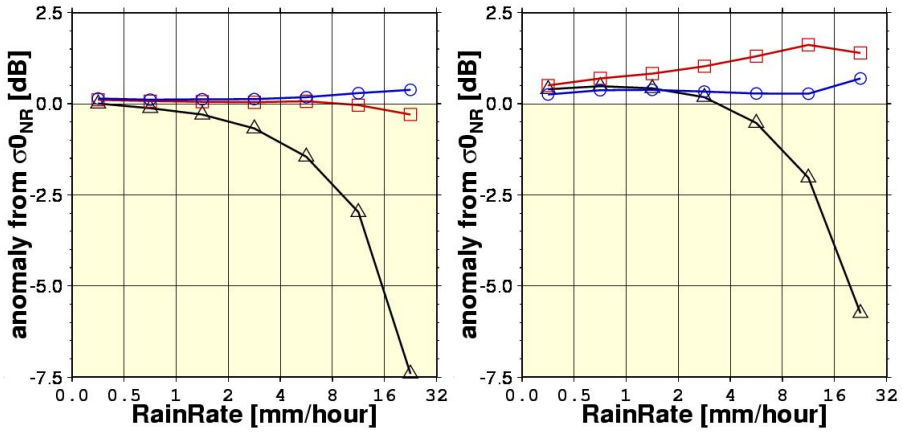

FIG. 1. $\Delta\sigma^0_R$ (triangle, black), $\Delta\sigma^0_{ref}$ (circle, blue), and $\Delta\sigma^0_{fin}$ (square, red) for the rain rate categories. The left panel is for ocean, and the right panel is for over land.

Surface type: ocean, land, and coast. Observations over coast is not treated in this study.

Rain flag: no-rain, rain-possible, and rain-certain. Rain-possible is regarded as no-rain.

Estimated surface rain rate: A new variable "e_SurfRain" is used. Up to version 5, the standard product gives "nearSurfRain", which is the rain rate at the lowest range bin free from ground clutter. In version 6, Z_m is extraporated into clutter region, then the rain rate is estimated at real surface range bin.

PIA: Path integrated attenuation. Both PIA_{ref} and PIA_{fin} are included in the 2A25 product. However PIA_{fin} is calculated only for the attenucation caused by precipitation. Attenuation by cloud water and water vapor are calculated and are added to PIA_{fin} for this analysis.

Observed surface cross section: σ^0_m (NR) or σ^0_m (R).

The incident angle θ is approximately calculated using angle bin number a as θ = 0.75 x | a-25 |. (1<=a<=49, 0<=θ<=18)

2.2. *Definition*

Using the data under rain conditions, three variables are defined as below.

$$\sigma^0_R=\sigma^0_m\ (R) \quad (10)$$

$$\sigma^0_{ref}=\sigma^0_m\ (R)+PIA_{ref} \quad (11)$$

$$\sigma^0_{fin}=\sigma^0_m\ (R)+PIA_{fin} \quad (12)$$

They are analyzed in the following sections 3 to 5, respectively.

σ^0_R should be less than σ^0_e (R) because σ^0_R involves the rainfall attenuation. σ^0_{ref} and σ^0_{fin} are estimates of σ^0_e (R). We would like to examine the anomaly of σ^0_e (R) from σ^0_e (NR), which is not known. σ^0_m (NR) are summarized for each surface type, incident angle, 1 by 1 degree grid and 1month, and the average is defined as σ^0_{NR}. σ^0_{NR} is used as the proxy of σ^0_e (NR). $\Delta\sigma^0$ indicates the anomaly of σ^0 from σ^0_{NR} as follows.

$$\Delta\sigma^0_R=\sigma^0_R-\sigma^0_{NR} \quad (13)$$

$$\Delta\sigma^0_{ref}=\sigma^0_{ref}-\sigma^0_{NR} \quad (14)$$

$$\Delta\sigma^0_{fin}=\sigma^0_{fin}-\sigma^0_{NR} \quad (15)$$

3. σ^0_R

3.1. Results

$\Delta\sigma^0_R$ for different rain rate categories are shown in Fig. 1 ($\Delta\sigma^0_{ref}$ and $\Delta\sigma^0_{fin}$ in this figure are described later). For the weakest rain rate, $\Delta\sigma^0_R$ is almost zero over ocean, but it is slightly positive over land. Over land, $\Delta\sigma^0_R$ keeps positive up to 4mm/h rain. For these weak to moderate rainfall, $\Delta\sigma^0_e$ (R)= σ^0_e (R) $-\sigma^0_{NR}$ is positive. In other words, σ^0_e is higher under rain condition than under no-rain condition. The map for $\Delta\sigma^0_R$ under weak rainfall (rain rate is less than 1mm/h) is shown in Fig. 2. Less vegetated area such as the Sahel of Africa, India, Australia, and south-western America have positive $\Delta\sigma^0_R$. In the tropical rainforest such as Amazon,

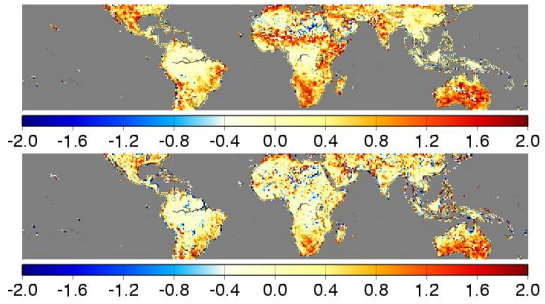

Fig. 2. $\Delta\sigma^0_R$ (upper) and $\Delta\sigma^0_{ref}$ (lower) under weak rainfall less than 1mm/h over land.

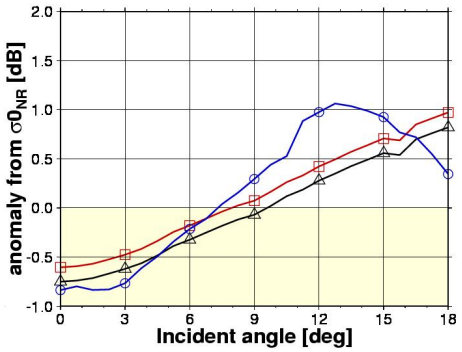

Fig. 3. $\Delta\sigma^0_R$ (triangle, black), $\Delta\sigma^0_{ref}$ (circle, blue), and $\Delta\sigma^0_{fin}$ (square, red) for different incident angles under weak rainfall less than 1mm/h over ocean.

$\Delta\sigma^0_R$ is almost zero.

The incident angle dependence of $\Delta\sigma^0_R$ for over-ocean under weak rainfall (rain rate is less than 1mm/h) is shown in Fig. 3. $\Delta\sigma^0_R$ is positively dependent on the incident angle. $\Delta\sigma^0_R$ is zero at approximately 10 degree. At larger than 10 degree, $\Delta\sigma^0_e$ (R) is higher under rain condition. At smaller incident angles, $\Delta\sigma^0_e$ (R) may be lower under rain condition.

3.2. Possible mechanism

The change of σ^0_e under rain condition can be explained as follows.

Over land, σ^0_e increases because surface becomes wet due to rainfall. It is known that the increase of soil moisture content increases the surface backscattering cross section. The sensitivity of σ^0_e on the soil moisture content is limited if the surface is covered by vegetation. This corresponds with the fact that $\Delta\sigma^0_R$ is almost zero in tropical rainforests.

Over ocean, the incident angle dependence of σ^0_e becomes weak due to stronger wind accompanied with rainfall. Previous researches show that the dependence of σ^0_e on the wind speed is almost zero around 10 degree. This corresponds with the result shown in Fig. 3.

These are mere hypotheses, as we do not have any observational proof. However, we are sure that this can partly explain the change of σ^0_e. According to the hypotheses, we called the phenomena that σ^0_e increases over land under rain condition as surface wetness effect. Similarly, the phenomena that the incident angle dependence of σ^0_e is weaken over ocean is called as wind speed effect

4. σ^0_{ref}

σ^0_{ref} is analyzed in this section. σ^0_{ref} is estimates of σ^0_e (R) by SRT. It is focused on that the σ^0_{ref} can explain the surface wetness effect and the wind speed effect.

4.1. General results

$\Delta\sigma^0_{ref}$ for different rain rate categories are shown in Fig. 1. Over land, $\Delta\sigma^0_{ref}$ is positive for all the categories. This indicates that the surface wetness effects are in some degree explained. However, $\Delta\sigma^0_{ref}$ is smaller than $\Delta\sigma^0_R$ for weak rainfall. This leads to negative PIA_{ref} because of the below equation.

$$PIA_{ref}=\sigma^0_{ref}-\sigma^0_R=\Delta\sigma^0_{ref}-\Delta\sigma^0_R . \quad (16)$$

σ^0_{ref} is underestimated at least for this case. The map of $\Delta\sigma^0_{ref}$ under weak rainfall (rain rate is less than 1mm/h) is shown in Fig. 2. In the Sahel and India, where show large surface wetness effects, $\Delta\sigma^0_{ref}$ is zero or slightly positive, and is much smaller than $\Delta\sigma^0_R$. On the other hand, in Australia, $\Delta\sigma^0_{ref}$ is comparable to $\Delta\sigma^0_R$.

The incident angle dependence of $\Delta\sigma^0_{ref}$ over ocean under weak rainfall (rain rate is less than 1mm/h) is shown in Fig. 3. $\Delta\sigma^0_{ref}$ is maximum at the incident angles around 12 to 15 degree. $\Delta\sigma^0_{ref}$ is smaller than $\Delta\sigma^0_R$ at 0 to 3 and near 18 degree. SRT over ocean does not follow the wind speed effect well.

4.2. over land

The reason why SRT over land can follow the surface wetness effect in some cases and the reason why this technique can not quantitatively follow the surface wetness effect are examined in more detail. In the standard algorithm for over-land, two methods are applied; along-track spatial reference method and temporal reference method. The former takes eight no-rain samples just prior to the current observation. TRMM always flies from west to east, thus the sample are taken outside and west of rain area. On the other hand, the latter takes no-rain samples within the 1 by 1 degree grid box same as the target pixel and in previous month. Of course, the incident angle and surface type of sample pixels should be the same as those of the target pixel. Between two estimates, one with smaller standard deviation of samples is chosen. Roughly speaking, along-track spatial reference method is chosen in 80 % cases.

In the along-track spatial reference method, samples are taken from no-rain area neighboring rain system. The characteristics of σ^0_m (NR) in such area are investigated. Figure 4 shows the relationship between $\Delta\sigma^0_m$ (NR)= σ^0_m (NR) -σ^0_{NR} and the distance (the number of pixels) to the neighboring rain area. The distance is calculated in along-track direction. The west side and the east side are discriminated. Within 10 pixels from the rain area, $\Delta\sigma^0_m$ (NR) is positive and it becomes higher by approaching to rain area. In the area neighboring to rain system, it might rain temporally just before with relatively high possibility. This can be the cause of the positive $\Delta\sigma^0_m$ (NR) in the neighboring area. Although the along-track spatial reference method basically takes samples in the neighboring area, the temporal reference method does not. Figure 5 is same as Fig. 1, but only in case of temporal reference method. $\Delta\sigma^0_{ref}$ is slightly negative, thus surface wetness effect is not explained at all in temporal reference method.

Asymmetry of $\Delta\sigma^0_m$ (NR) between the west side and the east side is seen in some regions. If the rain system moves from the west to the east, $\Delta\sigma^0_m$ (NR) can be higher in the west side, but not in the east side. In mid latitudes, where the westerlies is distinguished, $\Delta\sigma^0_m$ (NR) is higher in the west side.

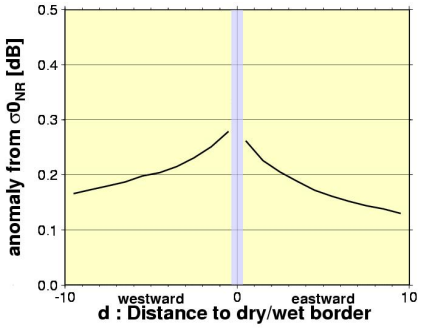

Fig. 4. $\Delta\sigma^0_m$ (NR) for the distance to the neighboring rain system over land.

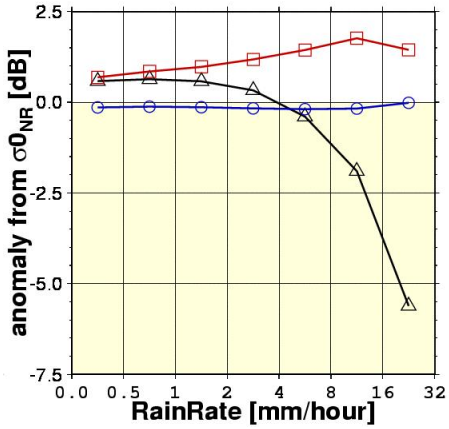

Fig. 5. The same as the right panel of Fig. 1, but for the case of temporal reference method.

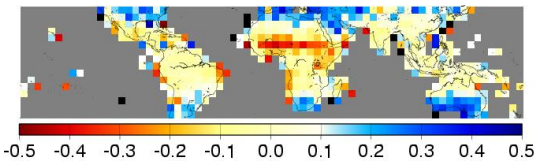

Fig. 6. The difference between $\Delta\sigma^0_m$ (NR) for the west side and that for the east side. Blue color indicates where $\Delta\sigma^0_m$ (NR) of the west is higher and red color indicates $\Delta\sigma^0_m$ (NR) of the east is higher.

On the other hand, in the Sahel, $\Delta\sigma^0_m$ (NR) is higher in the east side. However, in the standard algorithm, samples are taken in no-rain area outside and west of the rain system This may be the reason that the surface wetness effect is not explained in the Sahel even if the along-track spatial reference method is applied.

4.3. over ocean

Hybrid spatial reference method is applied if the entire scan is over ocean. For each pixel, σ^0_e is prepared by using σ^0_m for no-rain pixel and σ^0_{ref} by along-track spatial reference method for rain pixels. Then, σ^0_e is expressed by quadratic function of the incident angle θ. This fitting procedure yields the bias in σ^0_{ref}. If land or coast pixels exist in the scan, along-track or temporal reference method is applied same as over land. When the along-track spatial reference method is applied, $\Delta\sigma^0_{ref}$ is almost parallel to $\Delta\sigma^0_R$ (Fig. 7).

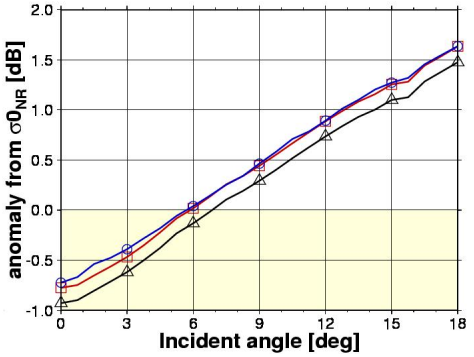

Fig. 7. The same as the Fig. 3, but for the case of along track spatial reference method.

5. σ^0_{fin}

σ^0_{fin} is another estimates of σ^0_e (R). As contrasted to σ^0_{ref}, to estimate σ^0_{fin}, observed Z_m and σ^0_m of the target pixel can be used. Moreover, σ^0_{fin} is always larger than σ^0_R. Judging from these points, σ^0_{fin} should be more reliable than σ^0_{ref} .

Over ocean, $\Delta\sigma^0_{fin}$ is always zero in Fig. 1. In Fig. 3, the incident angle dependence of $\Delta\sigma^0_{fin}$ for weak rainfall is parallel to that of $\Delta\sigma^0_R$. The incident angle where $\Delta\sigma^0_{fin}$ is zero is around 8 degree. For moderate to heavy rainfall, the incident angle dependence of σ^0_{fin} is deviated because biased σ^0_{ref} is relied on in the hybrid method.

Over land, $\Delta\sigma^0_{fin}$ has positive dependence on the rain rate (Figure 1). This is same in the case of temporal reference method (Figure 4). Careful analysis is required to judge that this dependence is the result of some physical phenomena.

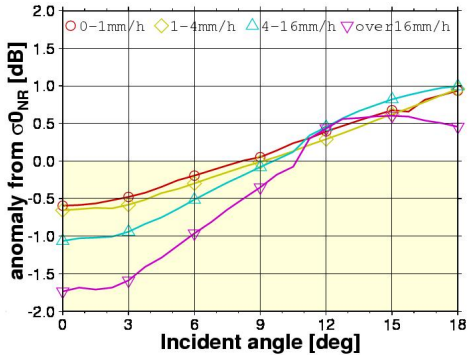

Fig. 8. The incident angle dependence of $\Delta\sigma^0_{fin}$ for various rain rate categories.

6. MODIFICATION OF SRT OVER LAND

The reasons for the lack of explanation of surface wetness effect over land are that temporal reference method is used and that sampling is always taken outside and west of the rain system. In order to overcome this weakness, modified SRTs are tested. In this section, the data in July 2001 are used.

Five modified SRTs are tested with the original SRT. All of them always apply along-track spatial reference method. WT takes eight samples prior to the observation (the west side) same as the standard algorithm, but ET takes eight samples posterior to the observation (the east side). Other three methods choose WT or ET each time. S1 applies WT if the target pixel is in the west half of rain area and applies ET if the target is in the east half of rain area. S2 chooses the method where the total distances from the target to the samples are shorter. S3 chooses the method that has smaller standard deviation of samples.

σ^0_{ref} from the five modified methods and the original method are compared in Fig. 9. By replacing the temporal reference method with the spatial reference method, the surface wetness effect can be partly explained. For the entire region, WT can follow the surface wetness effect compared with ET. S3 is similar to ET. This suggests that choosing smaller standard deviation contradicts with the explanation of the surface wetness effects. In the Sahel, ET is better than WT, as is expected from the result of Section 4.

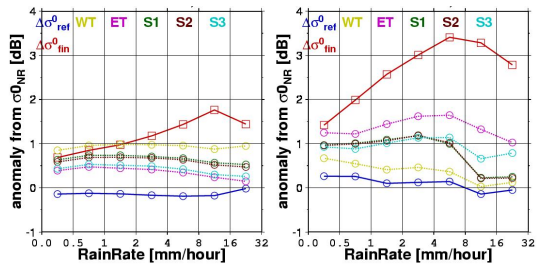

Fig. 9. $\Delta\sigma^0_{ref}$ for five modified SRT and the original SRT and the original $\Delta\sigma^0_{fin}$ for different rain rate categories. The left panel is for all the pixels where the temporal reference method is applied in the original. The right panel is for all the pixels in the Sahel (10-15N, 10-15E).

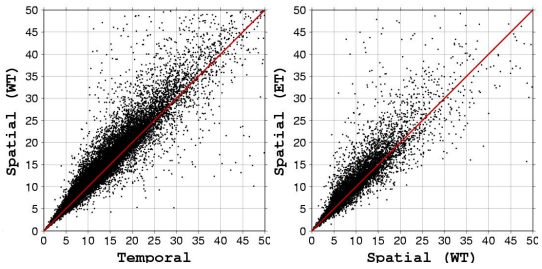

Fig. 10. Comparison of rain rate estimates from different SRTs. Left panel is for the pixels where the temporal reference method is originally applied. The ordinate is for the original case and the abscissa is for the cases applying spatial reference method (WT). Right panel is for the pixels in the Sahel (10-15N, 10-15E). The ordinate is for the cases applying spatial reference method (WT) and the abscissa is for the cases applying spatial reference method (ET).

The final rain rate estimates are significantly changed by the replacing SRT methods (Fig. 10). Applying the along-track spatial reference method instead of the temporal reference method, rain rate estimates tend to increase. In the Sahel, the rain rate estimates from the SRT of ET are generally higher than that from the SRT of WT. The effect is larger for heavy rainfall than for weak rainfall.

7. SUMMARY

Comparing the observed backscattering coefficients between under rain and no-rain conditions, it is found that over less vegetated land, σ^0_m under weak rainfall is statistically higher than σ^0_m under no-rain condition. This suggests that σ^0_e is higher under rain conditions than under no-rain condition. This increase of σ^0_e can be partly explained by the increase of surface wetness as a result of rainfall (surface wetness effect). Over ocean the incident angle dependence of σ^0_e is weaken under rainfall probably due to the increase of wind speed (wind speed effect).

Surface reference estimates σ^0_{ref} by the standard algorithm can follow the surface wetness effect and the wind speed effect in some degree particularly by the along-track spatial reference method. Temporal reference method does not explain the surface wetness effect at all, and hybrid spatial reference method yields the bias in the incident angle dependence of σ^0_e. Along-track spatial reference method does not work well in the Sahel compared with in the mid latitude. It can be because the samples are always taken outside and west of rain area.

Modified SRTs are applied. By replacing temporal reference method with spatial reference method, the surface wetness effect becomes partly explained. In the Sahel, by taking samples not west of but east of rain system, the estimated σ^0_e seems to be improved. The change of SRT also affects on the final rain rate estimates especially for heavy rainfall.

Acknowledgements. This study is part of a larger study, "Production of a high-precision, high-resolution global precipitation map using satellite data (GSMaP)" led by Prof. Ken'ichi Okamoto (Osaka Prefecture University, Japan) under the program, "Core Research for Evolutional Science and Technology (CREST)" of the Japan Science and Technology Agency (JST).

REFERENCES

Iguchi, T., *et al.*, 2000: Rain-profiling algorithm for the TRMM precipitation radar. *J. Appl. Meteor.*, **39**, 2038-2052.

Meneghini, R. et al., 2000: Use of the surface reference technique for path attenuation estimates from the TRMM precipitation radar. *J. Appl. Meteor.*, **39**, 2053-2070.

Meneghini, R., et al., 2004: A hybrid surface reference technique and its application to the TRMM Precipitation Radar. *J. Atmos. Oceanic Technol.*, **21**, 1645-1658.